Photoelectron Spectroscopy with Variable Photon Energy: A Study of the Metal Hexacarbonyls, $M(CO)_6$, Where M = CR, MO, and W

Glyn Cooper,[†] Jennifer C. Green,*[†] Martin P. Payne,[†] Barry R. Dobson,[‡] and Ian H. Hillier[‡]

Contribution from the Inorganic Chemistry Laboratory, Oxford 0X1 3QR, U.K., and the Chemistry Department, Manchester University. Manchester M13 9PL, U.K.
Received December 11, 1986

Abstract: Relative partial photoionization cross sections have been measured over the photon energy range 16–115 eV for the valence bands (6–20 eV binding energy) of free CO and the metal hexacarbonyls $Cr(CO)_6$, $Mo(CO)_6$, and $W(CO)_6$. All three transition-metal compounds show a very pronounced increase in intensity of the predominantly metal d orbital ionization bands (t_{2g}^{-1}) at photon energies ($h\nu$) corresponding to *n*p absorption ($Cr(CO)_6$, $h\nu$ = 52.5 eV, n = 3; $Mo(CO)_6$, $h\nu$ = 48 eV, n = 4; $W(CO)_6$, $h\nu$ = 44 and 53 eV, n = 5). The other valence bands show small intensity increases at similar energies. The origins of these and other features of the cross section variations with photon energy are discussed and compared with Hatree–Slater central field calculations of metal atom d orbital cross sections and our experimental results on free CO. Maxima in the d-band relative partial photoionization cross sections associated with a centrifugal barrier are identified for Cr and Mo ca. 23 and 26 eV photon energy, respectively. A further maximum at 42 eV in the d-band cross sections of $Cr(CO)_6$ is tentatively assigned to a shape resonance. The influence of Cooper minima in the 4d and 5d orbital cross sections of $Mo(CO)_6$ and $W(CO)_6$ is identified.

It is a common, though generally qualified, assumption in the interpretation of molecular photoelectron (PE) spectra that the molecular orbital (MO) photoionization cross sections are determined by the summation of atomic terms and that interference or overlap contributions may be neglected together with autoionization and resonance effects. As a result assignments of photoelectron bands and conclusions derived concerning bonding interactions have been heavily reliant on an empirical analysis of often subtle changes in intensity between the two standard He discharge lamp photon energies (He I, 21.2 eV; He II, 40.8 eV). In this regard, the Gelius model,[1] which strictly is only applicable in X-ray photoelectron spectroscopy (XPS), has been widely used. The use of synchrotron radiation allows the energy dependence of cross sections to be examined in detail and should enable the basis and limitations of such empirical intensity rules to be clarified. The observation of photoionization features such as resonance effects and Cooper minima[2] are in themselves potential sources of information on electronic structure and are of fundamental interest in connection with the theory of photon–matter interactions.

The photon energy dependence of differential cross sections is employed in photoemission experiments by using synchrotron radiation in order to disentangle the contributions from different atomic states to the valence band of compound solids.[3] In recent years, a considerable number of studies dealing with photoemission from transition metals, alloys, nonstoichiometric transition-metal compounds, and some simple transition-metal compounds such as chlorides and bromides have been reported.[4] However, although such solid-state studies allow suggestions to be made as to the contributions from different atomic orbitals to the valence band, severe overlapping of peaks does not allow a clear examination of the cross sections of individual orbitals.

In the work described below, the group VI metal hexacarbonyls, $Cr(CO)_6$, $Mo(CO)_6$, and $W(CO)_6$, are examined in the vapor phase by angle resolved photoelectron spectroscopy over a wide photon energy range. $Cr(CO)_6$ has been examined previously in the solid state,[5] but the spectra are of lower resolution, and the observations differ from ours. These compounds have been the subject of a wealth of spectroscopic[6] and theoretical studies,[7] providing a good understanding of their electronic structure. They therefore constitute a good testing ground for the usefulness of relative partial photoionization cross sections (RPPICS) as an interpretive tool in ultraviolet photoelectron spectroscopy (UPS) and as a source of electronic structural information. Because of the paucity of experimental data on transition-metal d-orbital ionization cross sections, these results on molecules with well-defined ion states should provide a useful test of theoretical models. In addition the present work is of interest in relation to the results of photoemission experiments on CO adsorbed on metal surfaces.[8] Some of the following results have been communicated briefly.[9]

Experimental Section

Synchrotron radiation from the 2-GeV electron storage ring at the SERC Daresbury Laboratory was monochromated by using a toroidal grating monochromator. Two gratings were employed in the photon energy ranges 10–50 eV (710 lines/mm) and 50–100 eV (2400 lines/mm). In order to maximize available signal, particularly in the high

[†] Inorganic Chemistry Laboratory.
[‡] Manchester University.

(1) Gelius, U. *Electron Spectroscopy*; Shirley, D. A., Ed.; North Holland, Amsterdam, 1972; p 311.
(2) Cooper, J. W. *Phys. Rev. Lett.* **1976**, *41*, 73.
(3) Eastman, D. E.; Freeouf, J. L. *Phys. Rev. Lett.* **1975**, *34*, 395.
(4) (a) Lenth, W.; Lutz, F.; Barth, J.; Kalkoffen, G.; Kunz, C.; *Phys. Rev. Lett.* **1978**, *41*, 1185. (b) Barth, J.; Gerken, F.; Kobayashi, K. L. I.; Weaver, J. H.; Sonntag, B. *J. Phys. C.* **1980**, *13*, 1369. (c) Sugawara, H.; Naito, K.; Miya, T.; Kakizaki, A.; Nagakura, I.; Ishii, T. *J. Phys. Soc. Jpn.* **1984**, *53*, 279. (d) Kakizaki, A.; Miya, T.; Naito, K.; Fukii, I.; Sugawara, H.; Nagakura, I.; Ishii, T. *J. Phys. Soc. Jpn.* **1985**, *54*, 3638.
(5) Loubriel, G.; Plummer, E. W. *Chem. Phys. Lett.* **1979**, *64*, 234.
(6) (a) Higginson, B. R.; Lloyd, D. R.; Burroughs, P.; Gibson, D. M.; Orchard, A. F. *J. Chem. Soc., Faraday Trans. 2* **1973**, *69*, 1659. (b) Trogler, W. C.; Desjardins, S. R.; Solomon, E. I. *Inorg. Chem.* **1979**, *18*, 2131. (c) Giordan, J. C.; Moore, J. H.; Tossell, J. A. *J. Am. Chem. Soc.* **1981**, *103*, 6632. (d) Jones, L. H.; Swanson, B. I. *Acc. Chem. Res.* **1976**, *9*, 128. (e) Plummer, E. W.; Salanek, W. R.; Miller, J. S. *Phys. Rev. B* **1978**, *18*, 1673. (f) Hubbard, J. L.; Lichtenberger, D. L. *J. Am. Chem. Soc.* **1982**, *104*, 5026.
(7) (a) Beach, N. A.; Gray, H. B. *J. Am. Chem. Soc.* **1968**, *90*, 5713. (b) Hillier, I. H.; Saunders, V. R. *Mol. Phys.* **1971**, *22*, 1025. (c) Caulton, K. G.; Fenske, R. F. *Inorg. Chem.* **1968**, *7*, 1273. (d) Baerends, E. J.; Ros, P. *Mol. Phys.* **1975**, *30*, 1735. (e) Johnson, J. B.; Klemperer, W. G. *J. Am. Chem. Soc.* **1977**, *99*, 7132. (f) Sherwood, D. E.; Hall, M. B. *Inorg. Chem.* **1980**, *19*, 1905. (g) Bursten, B. E.; Freier, B. G.; Fenske, R. F. *Inorg. Chem.* **1980**, *19*, 1810. (h) Yang, C. Y.; Arratia-Perez, R.; Lopez, J. P. *Chem. Phys. Lett.* **1984**, *107*, 112. (i) Ford, P. C.; Hillier, I. H. *J. Chem. Phys.* **1983**, *80*, 5664.
(8) (a) Yates, J. T., Jr.; Madey, T. E.; Campuzano, J. C. In *The Chemical Physics of Solid Surfaces and Heterogeneous Catalysis*; Vol. 3a, King, D. A., Woodruff, D. P., Ed.; Elsevier: Amsterdam 1985. (b) Peebles, D. E.; Peebles, H. C.; Bettan, D. N.; White, J. M. *Surf. Sci.* **1983**, *134*, 46. (c) Jensen, E. S.; Rhodin, T. N. *Phys. Rev. B* **1983**, *27*, 3338. (d) Freund, H. J.; Greuter, F.; Heskett, D.; Plummer, E. W. *Phys. Rev. B* **1983**, *27*, 7117.
(9) Cooper, G.; Green, J. C.; Payne, M. P.; Dobson, B. R.; Hillier, I. H. *Chem. Phys. Lett.* **1986**, *125*, 97.

0002-7863/87/1509-3836$01.50/0

photon energy region, the monochromator was used with fixed slit widths of approximately 2 mm. The resultant band pass of the monochromator varied from about 0.1 eV at the low-energy limit of each grating to 0.3 eV at the high-energy limit. For the measurements on CO the low-energy grating was employed up to 75 eV photon energy, since the lower resolution of this grating from 50 to 70 eV was not so critical. The gaseous samples were photoionized in a cylindrical ionization chamber. Photoelectrons were then energy analyzed by using a hemispherical analyzer of mean radius 65 mm operated at a constant pass energy of 6.4 eV for photon energies up to 50 eV and at a pass energy of 12.8 eV for photon energies above 50 eV. A three element zoom lens was used to accelerate or retard electrons prior to analysis, and a position sensitive multichannel detector[10] was used to increase sensitivity. (A full account of this apparatus and its performance is given elsewhere.[11]) Under the operating conditions outlined the electron energy analyzer contributed ca. 0.05 eV to photoelectron half widths. Bandwidths were therefore expected to be monochromator limited and to be in the range 0.1–0.3 eV. This was in agreement with measurements of full widths at half height of He $1s^{-1}$, Ar $3p^{-1}$, and Xe $5p^{-1}$ spectra.

In the present experimental arrangement the analyzer can be rotated in a plane at right angles to the incident photon beam and has an angular acceptance of ±2°. In order to determine relative partial photoionization cross sections, the analyzer was positioned at the "magic angle", so as to eliminate variations in intensity due to the photoelectron asymmetry parameter, β. The signal intensity as a function of angle is given by

$$\frac{d\sigma}{d\Omega} = \frac{\sigma}{4\pi}\left[1 + \frac{\beta}{4}(3P\cos 2\theta + 1)\right]$$

where σ is the cross section, θ the angle of the ionized electrons with respect to the principle electric vector of the elliptically polarized synchrotron radiation, P the degree of polarization of the photon beam, and Ω the acceptance angle of the analyzer. The polarization of the radiation was measured by using a four reflection polarization analyzer,[12] which gave P as 0.88 for a photon energy of 25 eV and a TGM band-pass of 0.05 eV. However, with the TGM band-pass settings and the large photon energy range used in these experiments, it was found more convenient to determine P from measurements on photoelectron spectra of Ar and He.[13] A β value of 2 was assumed for the He $1s^{-1}$ ionization, while for the $3p^{-1}$ ionization of Ar values were taken from the literature.[14,15] Polarization was also found to be dependent on the condition of the storage ring beam, and it was decided to use 123.5° as the magic angle for all energies (assumed polarization 85%). In the worst case this was estimated to give an error of 3° from the true magic angle.

As the photon intensity of the storage ring beam decayed with time, the scan rate at each radiation energy was linked to the output of a photomultiplier which intersected the photon beam after the latter had passed through the gas cell. However, the resulting experimental data had to be corrected for the fact that the photomultiplier showed a variable sensitivity to different photon energies. Calibration of the photomultiplier sensitivity was achieved by measurement of the np^{-1} ionizations of the noble gases Ne, Ar, and Xe, for which photoionization cross sections have been reported.[16,17] The three photomultiplier calibration data sets obtained during data collection on the metal hexacarbonyls were within 5% of each other, and the uncertainty introduced into the RPPICS data presented below due to photon energy calibration errors is therefore small.

The shapes of the photomultiplier calibrations obtained from Ne, Ar, and Xe differed at photon energies <35 eV, revealing a reduction in analyzer sensitivity to electrons having kinetic energies (KE) <15 eV. Above this KE the intensities of the inert gas np^{-1} bands appeared unaffected by analyzer sensitivity. The wide range of np^{-1} IEs for Ne, Ar, and Xe enabled us to derive KE calibration factors for the analyzer/lens system. For example, comparing the photomultiplier calibrations factors for Ne and Ar at 33 eV yielded a kinetic energy calibration factor for 11.6 eV KE electrons (Ne has an IE of 21.4 eV; 33 − 21.4 = 11.6), the Ar $3p^{-1}$ band with a KE of 17.5 eV (33 − 15.5 = 17.5) being unaffected in intensity. Full combination of the three data sets enabled the reduction in analyzer sensitivity below 15 eV KE to be characterized. Below a KE of 10 eV, we found a 15–20% variation in the calibration factors, and this is likely to be the major source of error in the corresponding RPPICS data.

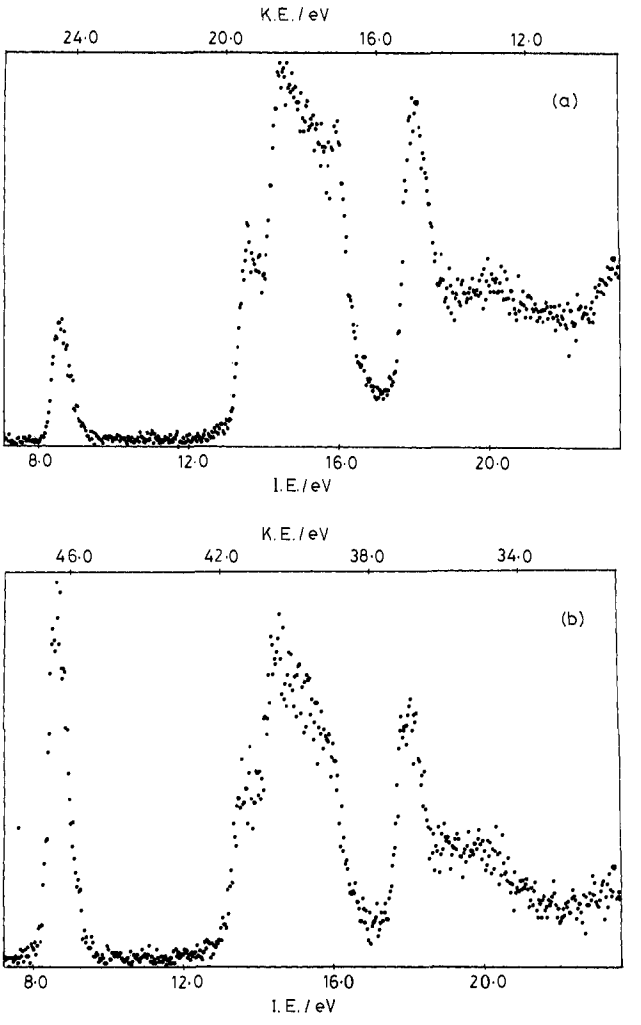

Figure 1. Photoelectron spectra of $Cr(CO)_6$ at (a) 33 eV and (b) 55 eV.

The hexacarbonyl samples were introduced into the ionization region by simply allowing them to sublime from a side-arm tube attached to the gas cell. Since there was no direct way of measuring pressure fluctuations of the samples, standard spectra, e.g., 30 eV photon energy, 12–20 eV scan width, were run between each data collection spectrum, and the intensities of the bands in these were used to correct for intensity variations with time. For $Cr(CO)_6$ and $Mo(CO)_6$ these proved considerable (25% over a 2–3-day period). It is estimated that errors of less than 5% were introduced into the RPPICS by this procedure.

As instrumental resolution varied as a function of photon energy, band areas rather than peak heights were used to determine intensities. In each case a linear background was subtracted from a band prior to integration Only for bands C are uncertainties in the background determination large enough to introduce considerable error into the calculated RPPICS. These are probably <5% for $Cr(CO)_6$ and $Mo(CO)_6$ and <10% for $W(CO)_6$.

The branching ratio data has been corrected with the kinetic energy calibration but is independent of the sensitivity of the photomultiplier to photon energy and the long term variation in sample pressure. Photoelectron branching ratios are not quoted for any band below 10 eV KE, owing to the uncertainty of the calibration in this region, so that integration errors are the most significant source of error for this data (see below). For the points on the RPPICS plots, where pressure variations and photomultiplier calibration factors also contribute to the possible errors, relative values of points within 5 eV of each other are probably accurate to within 5%, whereas data separated by >20 eV contain a relative uncertainty of 10%.

$Cr(CO)_6$, $Mo(CO)_6$, and $W(CO)_6$ were obtained from Strem Chemicals Inc. and were used without further purification. Their He I spectra (obtained on a PES Laboratories 0078 spectrometer) were checked against the literature reports.[6a]

(10) MacDowell, A. A.; Hillier, I. H.; West, J. B. *J. Phys. E: Sci. Instrum.* **1983**, *16*, 487.
(11) Potts, A. W.; Novak, I.; Quinn, F.; Marr, G. V.; Dobson, B.; Hillier, I. H.; West, J. B. *J. Phys. B* **1985**, *18*, 3177.
(12) Parr, A. C.; Stockbauer, R.; Cole, B. E.; Ederer, D. L.; Dehemer, J. L.; West, J. B. *Nucl. Instrum. Meth.* **1980**, *172*, 357.
(13) Derenbach, H.; Malutzki, R.; Schmidt, V. *Nucl. Instrum. Meth.* **1983**, *208*, 845.
(14) Holland, D. M. P.; Parr, A. C.; Ederer, D. L.; Dehemer, J. L.; West, J. B. *Nucl. Instrum. Meth.* **1982**, *195*, 331.
(15) Houlgate, R. G.; West, J. B.; Codling, K.; Marr, G. V. *J. Elec. Spectrosc. Relat. Phenom.* **1976**, *9*, 205.
(16) West, J. B.; Marr, G. V. *Proc. Roy. Soc. London A* **1976**, *349*, 397.
(17) West, J. B.; Morton, J. *At. Data Nucl. Data Tables* **1978**, *22*, 103.

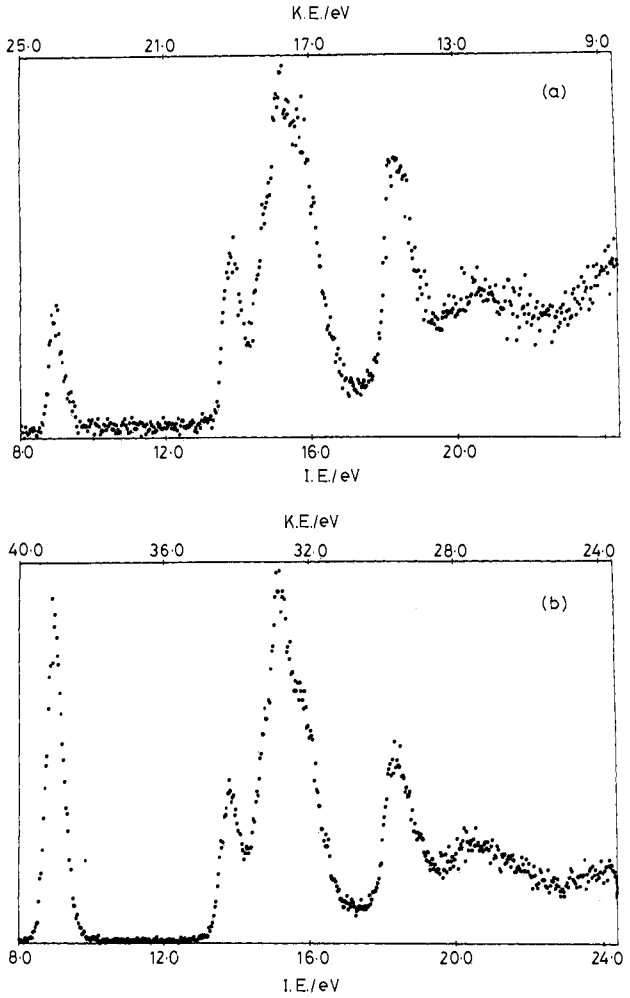

Figure 2. Photoelectron spectra of $Mo(CO)_6$ at (a) 33 eV and (b) 48 eV.

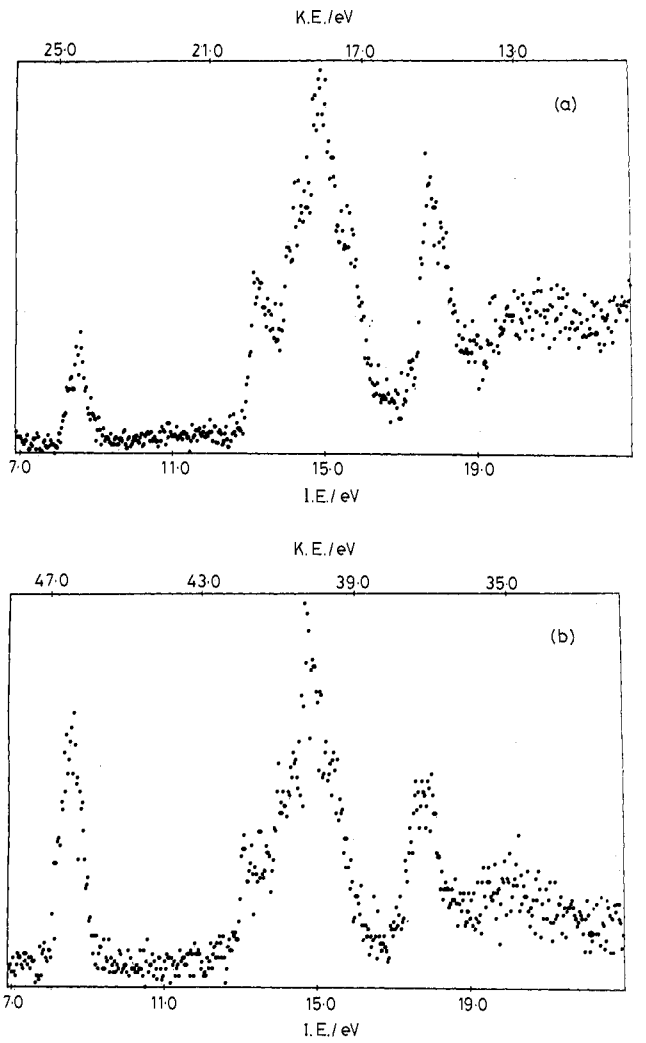

Figure 3. Photoelectron spectra of $W(CO)_6$ at (a) 33 eV and (b) 55 eV.

Results

Photoelectron spectra of $Cr(CO)_6$, $Mo(CO)_6$, and $W(CO)_6$, obtained at the magic angle, are shown in Figures 1–3. In each case the spectrum generated at low and "resonant" photon energy is shown, demonstrating relative intensity changes of the bands. Spectra at 33-eV photon energy are shown for $Cr(CO)_6$, $Mo(CO)_6$; and $W(CO)_6$ in Figures 1a, 2a, 3a, respectively; Figures 1b and 3b show the spectra of $Cr(CO)_6$ and $W(CO)_6$ at photon energy 55 eV, and Figure 2b that of $Mo(CO)_6$ at 48 eV.

The valence ionization processes in these compounds divide into three distinct categories; bands A are due to ionization from the t_{2g} MOs, which are predominantly metal d in character, bands B derive from MOs comprised largely of CO 1π and 5σ orbitals, while both components of bands C were originally assigned to ionizations from MOs of ligand 4σ character[6a] although bands C_2 have since been identified as shake up peaks associated with the $1\pi + 5\sigma$ levels.[18] A schematic MO diagram is given in Figure 4.

For $W(CO)_6$ 4f ionization bands were observed at 38.4 eV ($^2F_{7/2}$) and 40.7 eV ($^2F_{5/2}$), with photon energies from 70 to 110 eV.

RPPICS derived for bands A, B, and C for $Cr(CO)_6$, $Mo(CO)_6$, and $W(CO)_6$ are shown in Figures 5–7 and for the f-band of $W(CO)_6$ in Figure 8. Corresponding data on the 1π, 5σ, and 4σ bands of CO are given in Figure 9. Photoelectron branching ratios for the hexacarbonyls are shown in Figure 10.

The B bands of the hexacarbonyls were also divided into separate components, both by integration over four different areas of the bands and by fitting seven Gaussian curves of equal width.

(18) Rajona, D. S.; Kornat, L.; Plummer, E. W.; Salaneck, W. *Chem. Phys. Lett.* **1977**, *49*, 64.

Table I. Free Atom Subshell Binding Energies (eV) for the *n*p States of Cr, Mo, and W Referenced to the Vacuum Level[19] and Photon Energies of Maxima in the Photoionization Cross Sections as a Function of Photon Energy for $Cr(CO)_6$, $Mo(CO)_6$, and $W(CO)_6$

	atomic binding energies		$h\nu$ of PE cross section maxima		
	$np_{3/2}$	$np_{1/2}$	A	B	C
Cr, $n = 3$	48	49	52.5 ± 2	52.5 ± 2	52.5 ± 2
Mo, $n = 4$	42	45	48 ± 2	42 ± 1, 46.5 ± 1.5	
W, $n = 5$	41	51	44 ± 1, 53 ± 2	42 ± 1.5, 53 ± 2	

Although seven peaks can be identified within bands B in high resolution spectra, the separations were found to be more accurate and reproducible using four components. The four IE ranges for $Mo(CO)_6$ were as follows: B_1 12.71–13.80 eV, B_2 13.83–14.47 eV, B_3 14.50–15.14 eV, and B_4 15.17–16.60 eV. The results of this analysis are given in Figure 11. Similar ranges were defined by $Cr(CO)_6$ and $W(CO)_6$, but, since no significant differences in cross section behavior were found for these hexacarbonyls, the exact data are omitted here.

Discussion

Metal d Bands. Figures 5–7 and 10 show that there is a marked difference in the variation of photoionization cross sections with photon energy for the various valence band ionizations of the group VI metal hexacarbonyls. The A bands show, superimposed on a general slow fall in cross section with photon energy, large increases in intensity at energies close to the *n*p ionization energies

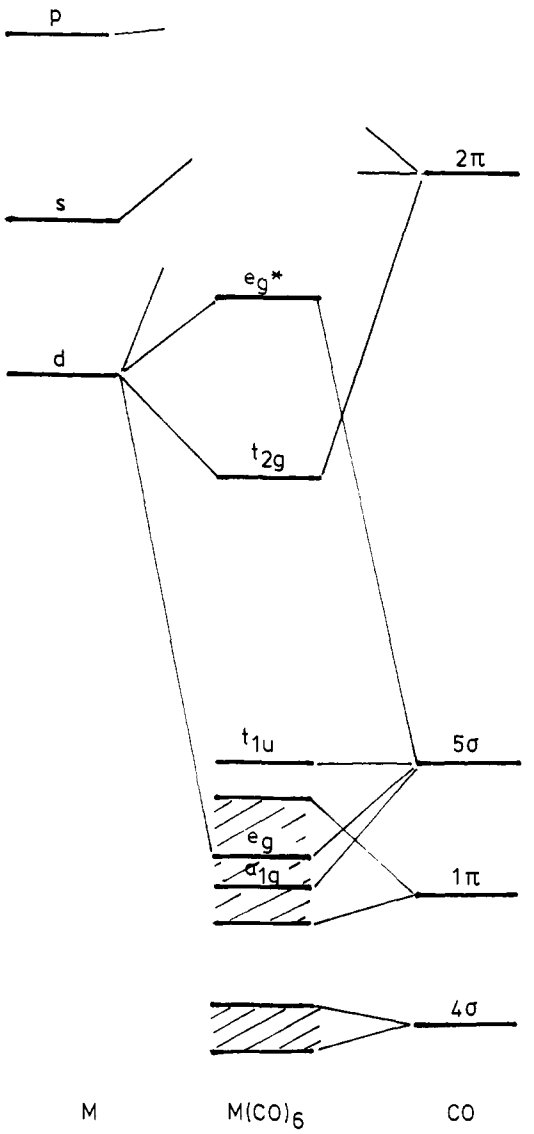

Figure 4. Schematic MO diagram for a Group VI hexacarbonyl.

of the free metal atoms. These energies and the maxima of the photoionization features are given in Table I. The proposition that the large intensity increases are associated with an *n*p excitation is made particularly compelling by the data on $W(CO)_6$, where two maxima are observed with a separation comparable to the spin–orbit splitting of the $5p^{-1}$ states of atomic tungsten.[19] A similar double-humped resonance was observed in a photoemission study of tantalum selenides.[20]

Resonant photoemission on excitation of inner shells has been observed for rare earth[4a] and transition metals.[4b] For d-block elements, it is attributed to the processes

$$np^6nd^x \xrightarrow{h\nu} np^5nd^{x+1} \rightarrow np^6nd^{x-1} + e \qquad (1)$$

where e represents an ionized electron. A *n*p → *n*d photoabsorption is followed by a super-Coster–Kronig decay with associated emission of a d electron. The kinetic energy of the ionized electron is such that in a photoemission experiment the emitted electrons are indistinguishable from those obtained by the direct process

$$np^6nd^x \xrightarrow{h\nu} np^6nd^{x-1} + e \qquad (2)$$

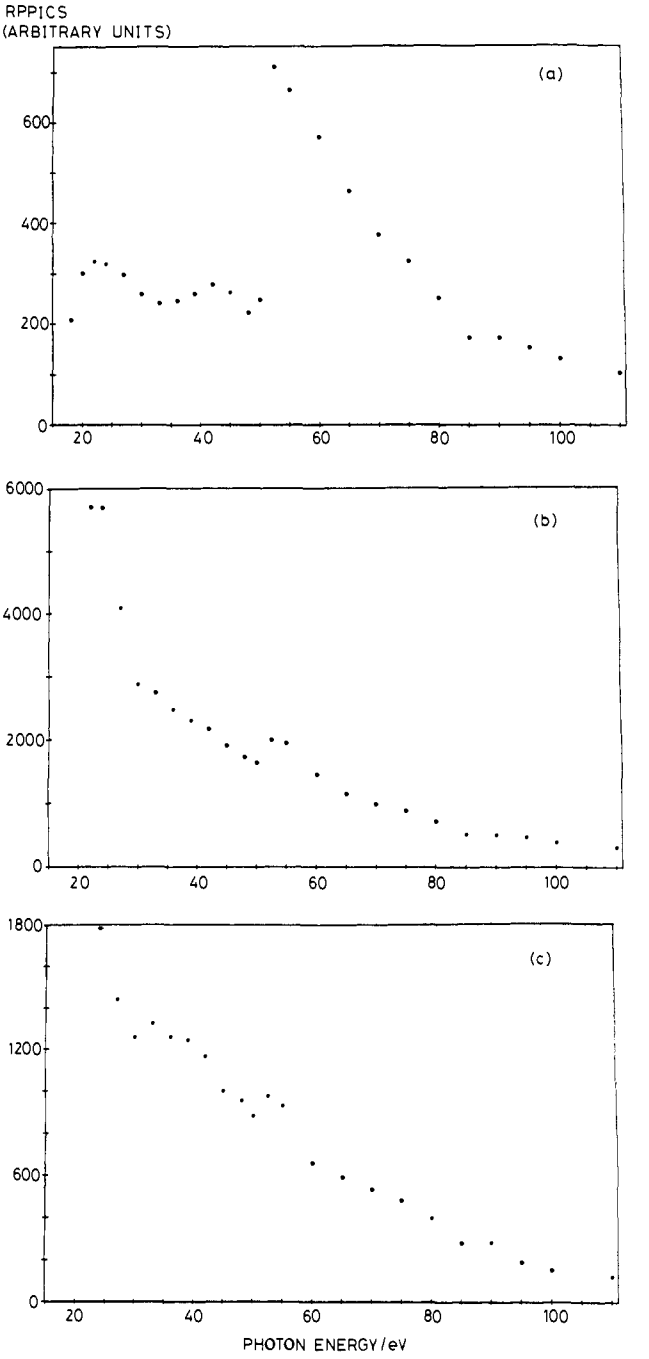

Figure 5. RPPICS as a function of photon energy for $Cr(CO)_6$: (a) band A, (b) band B, (c) band C.

Thus an enhancement of the *n*d band in the region of the *n*p absorption may be observed. In a photoabsorption experiment *n*p → *n*d transitions are observed as prominent absorption peaks.[21]

The necessary conditions for this type of resonant enhancement of photoionization intensity are as follows.[22] (1) The excited electron must be of high angular momentum (i.e., a d or f electron) such that it can exist in a quasi-bound state above the ionization potential in the inner well region of the combined attractive Coulomb and repulsive centrifugal potentials. (2) The *n*d shell must be partially filled. (3) The inner and outer shells must be of the same principal quantum number to ensure a sufficiently large overlap between the two orbitals and thus a large transition moment.

(19) *Handbook of X-ray and Ultraviolet Photoelectron Spectroscopy*; Briggs, D., Ed., Heyden: London, 1977.
(20) (a) Sakamoto, H.; Suga, S.; Taniguchi, M.; Kanzaki, H.; Yamamoto, M.; Seki, M. *Solid State Commun.* **1984**, *52*, 721. (b) Sato, E.; Ohtake, K.; Yamamoto, R.; Doyama, M.; Mori, T.; Soda, K.; Suga, S.; Endo, K. *Solid State Commun.* **1985**, *55*, 1049.
(21) (a) Zimkina, T. M.; Fomichev, V. A.; Gribovskii, S. A.; Zhukova, I. I. *Fiz. Tverd. Tela* **1976**, *9*, 1447; *Sov. Phys. Solid State* **1967**, *9*, 1128. (b) Starace, A. F. *Phys. Rev. B* **1972**, *5*, 1773.
(22) Dehmer, J. L.; Starace, A. F.; Fano, U.; Sugar, J.; Cooper, J. W. *Phys. Rev. Lett.* **1971**, *26*, 1521.

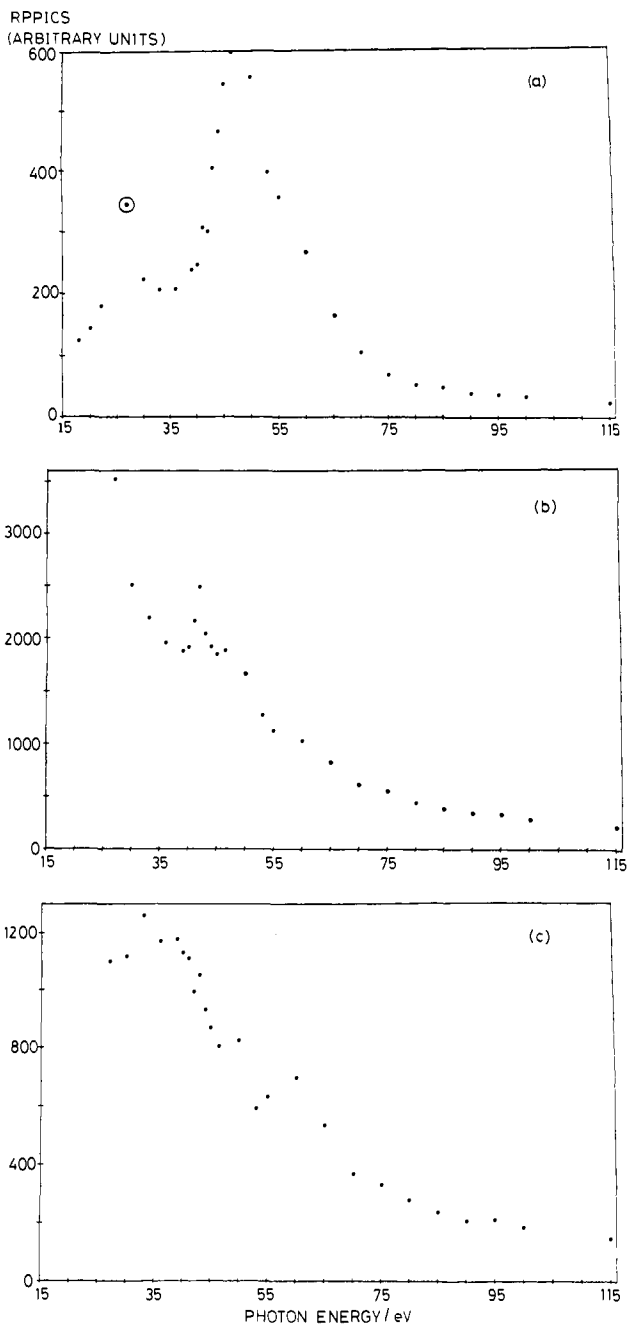

Figure 6. RPPICS as a function of photon energy for $Mo(CO)_6$: (a) band A, (b) band B, (c) band C.

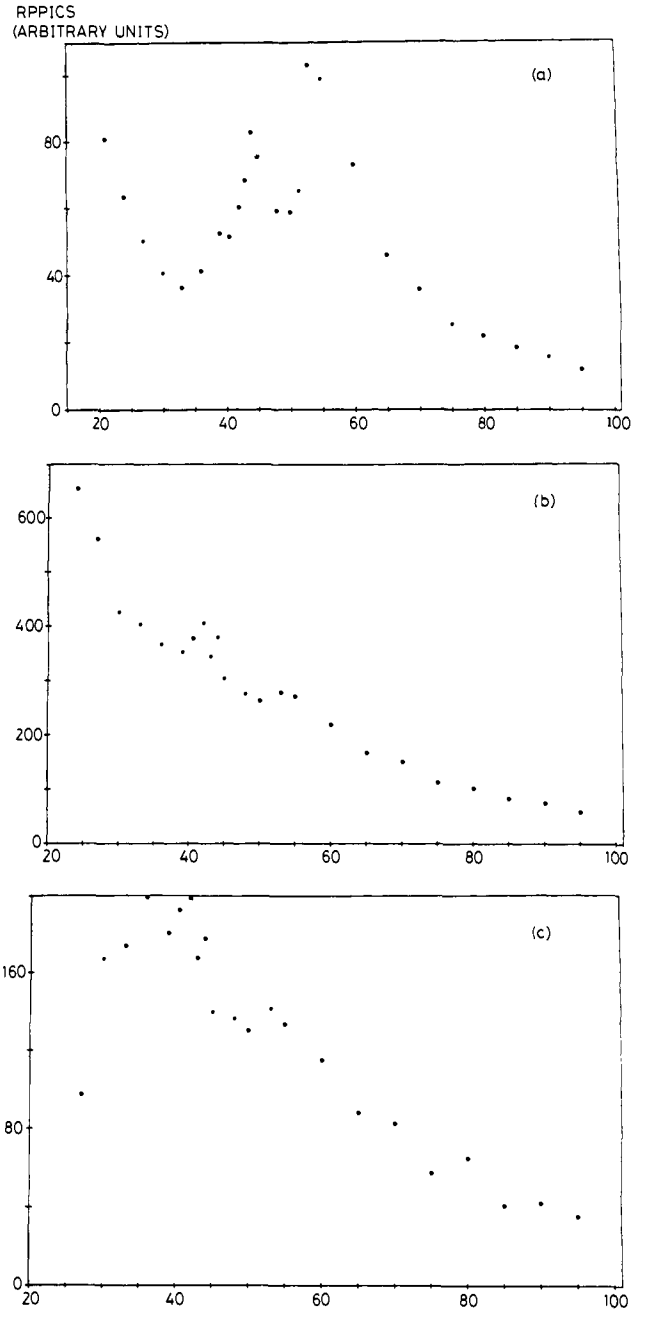

Figure 7. RPPICS as a function of photon energy for $W(CO)_6$: (a) band A, (b) band B, (c) band C.

Interference between processes 1 and 2 results in a Fano profile for the resonance,[23] represented by the formula

$$\sigma = \sigma_0 \frac{(q + \epsilon)^2}{(1 + \epsilon^2)} \qquad (3)$$

where $\epsilon = (E - E_r)/0.5T$, E_r is the resonance energy, T is the resonance width, q is the line profile index, and σ_0 is a background cross section, which is assumed to be constant over the width of the resonance. In this study $Cr(CO)_6$ gives the best example of such a profile with a minimum at 48.0 eV rising steeply to a maximum at 53.0 eV, followed by a slow decay over ca. 25 eV. In the absorption spectrum of $Cr(CO)_6$ a maximum has been observed at 49.0 eV.[24] We have performed a least-squares fit of resonance function 3, modified so that σ_0 varies linearly with photon energy, to the A band RPPICS of $Cr(CO)_6$. A satisfactory fit over the photon energy range 48–85 eV was obtained with $q = 1.4 \pm 0.1$, $E_r = 51.2 \pm 0.5$, $\sigma_0 = 260 \pm 15$, and $T = 11.5 \pm 0.1$. An estimation of the line profile index can also be obtained from the expression[4d]

$$q = \pm\gamma + (\gamma^2 + 1)^{1/2}$$

where the plus sign holds when $q > 1$ and the minus sign when $q < 1$, and $\gamma = \Delta h\nu_p/\Delta h\nu_h$. $\Delta h\nu_p$ is the energy separation of the minimum and maximum, and $\Delta h\nu_h$ is the full width at half height of the resonance peak. For $Cr(CO)_6$ $\Delta h\nu_p = 4.5$ and $\Delta h\nu_h = 15$, giving $q = 1.34$ or 0.744. The larger value compares favorably with the value of 1.4 ± 0.1 obtained from the fit.

Attempts were also made to fit the corresponding data on $Mo(CO)_6$ and $W(CO)_6$ by using two resonance energies (to take into account the spin–orbit splittings of the np^5 configurations), but good fits could not be obtained. This may be a result of nonlinear variations in σ_0 due to an approaching Cooper minimum in the 4d and 5d orbital cross sections (see below) or to shape resonances underlying the larger $np \rightarrow nd$ resonance. Another possibility is that exchange interactions between accessible states

(23) (a) Fano, U. *Phys. Rev.* **1961**, *124*, 1866. (b) Gerken, F.; Barth, J.; Kobayashi, K. L. I.; Kunz, C. *Solid State Commun.* **1980**, *35*, 179.
(24) Hayes, R. G. *Ann. Phys. Soc.* **1984**, *6*, 158.

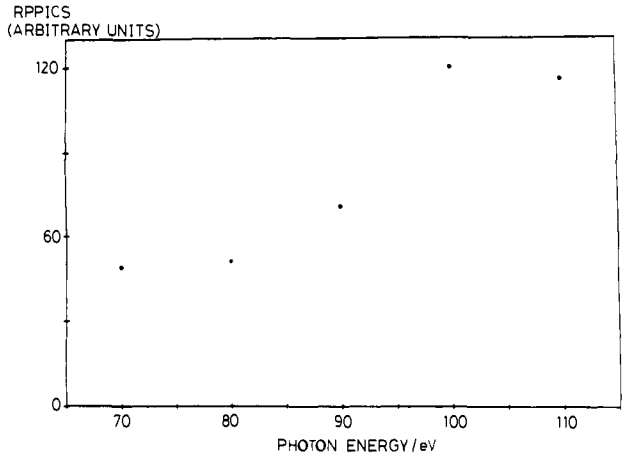

Figure 8. RPPICS as a function of photon energy for the f-band of $W(CO)_6$.

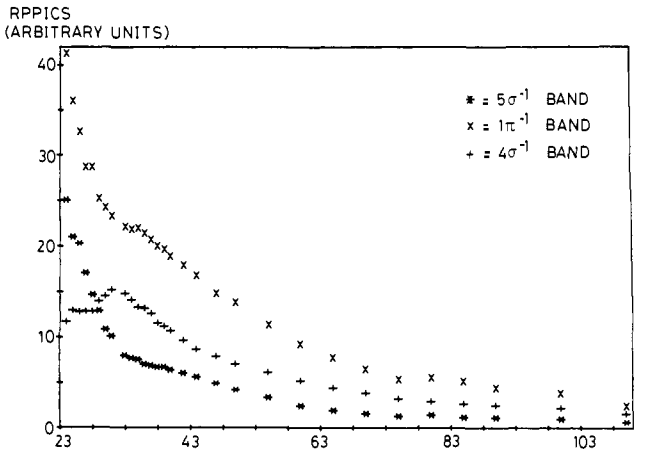

Figure 9. RPPICS as a function of photon energy for the 1π, 5σ, and 4σ of CO.

derived from the $p^5e_g{}^{*1}$ configuration may also complicate the profile.

In this context, we note that the two spin–orbit components of the $W(CO)_6$ p → d resonance do not have an intensity ratio of 2:1, as might be expected for the $p_{3/2}$:$p_{1/2}$ hole states. The $p_{3/2}$ state should have the lower excitation energy as the p shell is more than half-filled; however, it gives rise to the weaker of the two resonance peaks (see Figure 7a). In Table II we summarize the states arising from a $p^5e_g{}^{*1}$ configuration in octahedral symmetry, in two limiting cases: one where the spin–orbit splitting of the p shell is neglected and the exchange splitting is predominant, and one where the spin–orbit splitting is the more important perturbation. In the O* double group, the dipole selection rule determines that only Γ_4 states are accessible in the p → d excitation. In the first case the spin selection rule should also operate ensuring only the $^1T_{1u}$ state is reached. In the second case all three Γ_4 states may be accessible. The noncrossing rule leads the $^1T_{1u}$ state to correlate with the Γ_4 state arising from the $p_{1/2}$ term. The other two, which are associated with the $p_{3/2}$ term, correlate with states arising from spin–orbit splitting of the $^3T_{1u}$ and $^3T_{2u}$ states. In an intermediate situation where the spin–orbit splitting is sufficiently large to be observed but does not dominate totally the selection rules, the transition to $\Gamma_4(p_{1/2})$ will be fully allowed whereas those to the other $\Gamma_4(p_{3/2})$ states will still to some extent be less probable due to the operation of the spin selection rule. This may account for the relative intensities of the two $W(CO)_6$ resonances being less than the 2:1 ratio that might have been anticipated. A similar situation has been discussed by Wendin[25] for the 5d → 5f resonances of Th and U metal; in these cases the experimental profiles have been successfully compared with those

(25) Wendin, G. *Phys. Rev. Lett.* **1984**, *53*, 724.

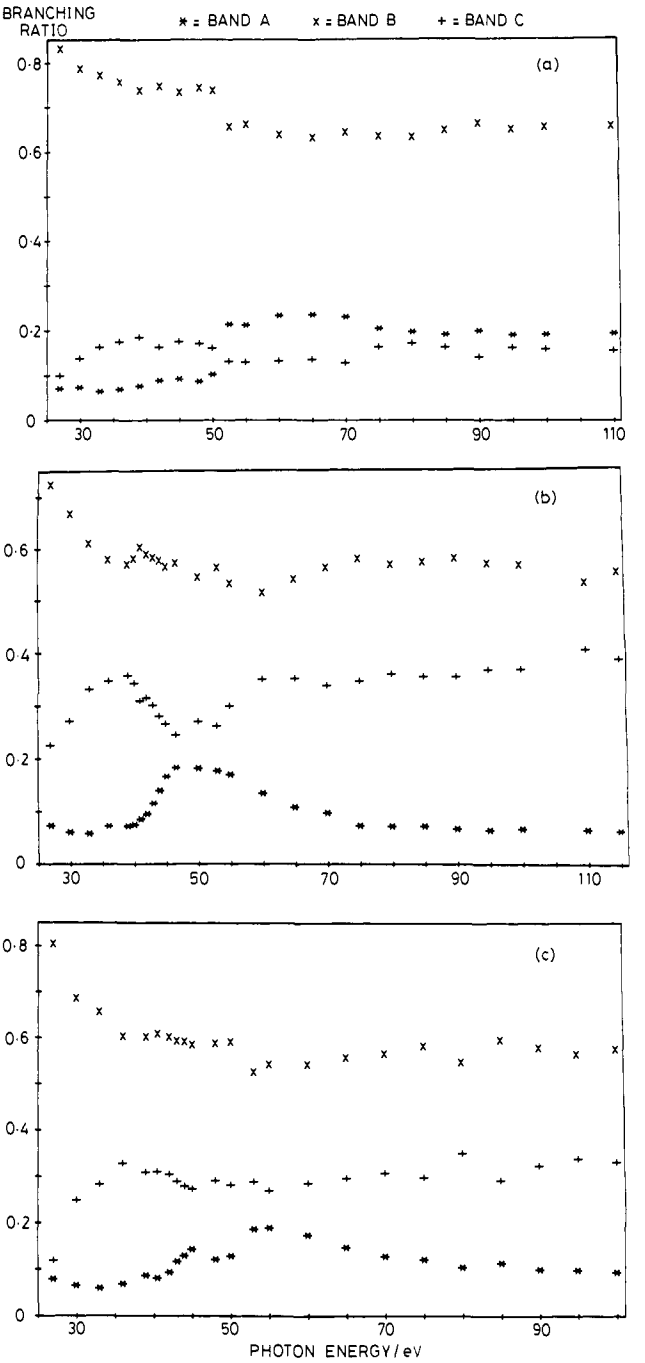

Figure 10. Photoelectron branching ratios for (a) $Cr(CO)_6$, (b) $Mo(CO)_6$, and (c) $W(CO)_6$.

Table II. States Arising from a $p^5e_g{}^1$ Configuration in an Octahedral Group in Exchange-Energy and Spin–Orbit Limits

exchange-splitting limit		spin-orbit limit
	$^1T_1 \rightarrow \Gamma_4$ $^1T_2 \rightarrow \Gamma_5$	$\Gamma_3 + \Gamma_4 + \Gamma_5 \leftarrow \Gamma_6 \times \Gamma_8$
$t_{1u}{}^5e_g{}^1$		
	$^3T_2 \rightarrow \Gamma_2 + \Gamma_3 + \Gamma_4 + \Gamma_5$ $^3T_1 \rightarrow \Gamma_1 + \Gamma_3 + \Gamma_4 + \Gamma_5$	$\Gamma_1 + \Gamma_2 + \Gamma_3 \leftarrow \Gamma_8 \times \Gamma_8$ $2 \times \Gamma_4 + 2 \times \Gamma_5$
		$e_g{}^1 = \Gamma_8$; $t_{1u}{}^5 = \Gamma_6 + \Gamma_8$
	Selection Rules $t_{1u}{}^6e_g{}^0 \rightarrow t_{1u}{}^5e_g{}^1$	
	$^1A_{1g} \rightarrow {}^1T_{1u}$	$\Gamma_1 \rightarrow \Gamma_4$

predicted by a local-density-based random-phase approximation.

Although the RPPICS plots for the *n*d bands are dominated by the *n*p → *n*d resonances, other features are also apparent. For

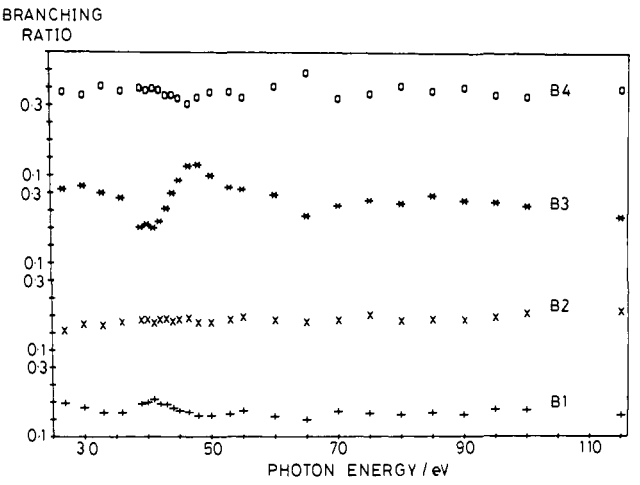

Figure 11. Branching ratios for the four components of the B band, B_1–B_4.

$Cr(CO)_6$, at low-photon energies, there is an increase in cross section with photon energy. The RPPICS plot passes through a maximum at ca. 23 eV after which it drops to a minimum at ca. 32 eV, followed by a second, though lower maximum at ca. 42 eV. For $Mo(CO)_6$ an initial increase in cross section of the d band is also observed for the first few data points; a maximum ca. 26 eV is somewhat obscured by a rogue point at 27 eV. No second maximum is found, however, perhaps because the p → d resonance photon energy is somewhat lower for $Mo(CO)_6$ than $Cr(CO)_6$. In the case of $W(CO)_6$ in the low-photon energy region there is a decline in ionization cross section with increasing photon energy. If any maximum occurs it must lie at lower $h\nu$ than those used for these observations. Again, the region around 40 eV, where a maximum occurs for $Cr(CO)_6$, is dominated by the large p → d resonance.

The main channel for ionization of d electrons is via a free electron f wave.[26] The effective potential experienced by an electron in an atom can be approximated by the central field potential[27]

$$\frac{-Ze^2}{r} + \frac{l(l+1)}{r^2}$$

where Z the effective nuclear charge varies with distance from the nucleus r, and l is the angular momentum of the electron. The second term is the repulsive centrifugal potential which prevents electrons, other than s electrons, for which $l = 0$, approaching the nucleus. For f electrons the effective potential can possess two minima; one in the outer region of the atom, where the attractive coulombic potential is hydrogen-like, and a second in the inner region, where the wave function penetrates the core. The intervening maximum can have a positive potential and occurs just prior to core penetration. Due to this intermediate range maximum, at low photoelectron energies, a continuum f wave function does not penetrate into the atom (where the d electron has most of its amplitude) and the ionization dipole matrix element is low. Only at higher energies does penetration by the f wave become effective. In consequence there is an increase in d orbital photoionization cross section with photon energy from threshold. At high energies the continuum wave function continues to move in toward the nucleus and becomes oscillatory, so that cancellation of positive and negative terms in the dipole matrix element then causes a decrease in cross section. The cross sections of *n*d electrons (and especially of *n*f electrons for which the barrier is even higher) are therefore low near threshold and rise to a maximum some eV above threshold. We associate the maxima at 23 eV ($Cr(CO)_6$) and 26 eV ($Mo(CO)_6$) (corresponding to kinetic energies of 14.5 and 17.5 eV, respectively) with these centrifugal barrier effects. The presumed maximum for $W(CO)_6$ may occur at photon energies <20 eV.

The central field calculations of Lindau et al.[28] predict maxima at kinetic energies of 16.5 ± 5, 15 ± 2, and 12 ± 2 eV for atomic Cr, Mo, and W (corresponding to photon energies of 25, 23.5, and 20.5 eV). These values are seen to be close to those observed experimentally for the hexacarbonyls. However, more sophisticated calculations, e.g., Hartree–Fock calculations, which treat electron exchange more rigorously, will tend to shift these barrier maxima to higher KE.[29,30] The bonding interactions of the *n*d orbitals in a hexacarbonyl are seen to reduce the centrifugal barrier maximum. One possible mechanism for this is that the d orbitals, in bonding to the CO ligands, effectively become more diffuse, so that penetration into the metal electron density by the continuum f wave function occurs at larger distances, thereby reducing the height of the intermediate range potential maximum.

We also assign the rise in cross section of the 4f bands of $W(CO)_6$ between 70 and 100 eV as due to a centrifugal barrier effect. The barrier is higher and more extended for molecular f electrons as the angular momentum of the free electron wave is higher than for the d ionizations.

The maximum in the RPPICS plot for $Cr(CO)_6$ at 42 eV may be associated with a shape resonance.[31] Similar features may be present in the RPPICS of $Mo(CO)_6$ and $W(CO)_6$, the large p–d resonances preventing their clear observation.

The final feature of the RPPICS plots of the d-bands on which we wish to comment is the more steep falloff at high photon energies for $Mo(CO)_6$ and $W(CO)_6$ than for $Cr(CO)_6$. Unlike Cr 3d orbitals, Mo 4d and W 5d orbitals possess radial nodes; consequently, their photoionization cross sections are expected to show Cooper minima. The predicted positions of these minima are 90 eV for atomic Mo and ca. 200 eV for the first minimum of atomic W.[28] Chromium 3d ionization cross sections, on the other hand, are not expected to display a Cooper minimum, and so exhibit a much slower decline in cross section with photon energy. Though the extent of our measurements is insufficient to identify any actual minima, we attribute the low cross sections at high photon energies for the Mo and W compounds to this phenomenon. Minima have been found in the 4d cross section of Mo metal at 200 eV and of MoS_2 at 110 eV.[32]

Ligands Bands and Gaseous CO. The B bands show a general decrease in photoionization cross section with photon energy, similar to those found above 25 eV for the 1π and 5σ bands of CO gas (see Figure 9). Photoionization cross sections of the valence bands of CO have been measured previously by several authors, the published data encompassing the photon energy range 15–50 eV.[33] Our measurements are in reasonable agreement and extend the range up to 110 eV. The fractional rate of decrease is markedly reduced above 80 eV, and no resonance features are observed. The small apparent increase in cross section of the 1π orbital at 80 eV we attribute to systematic errors in calibration factors that become apparent on a change of gratings.

In the RPPICS of the B bands of the hexacarbonyls small resonance features not present in the CO RPPICS are also observed. The energies of their maxima are given in Table I. They may be divided into two types, those which are associated with the metal t_{2g}^{-1} resonances (i.e., at the same $h\nu$) and those which are not. The former show that the excitation

$$np^6t_{2g}^6e_g^{*0} \xrightarrow{h\nu} np^5t_{2g}^6e_g^{*1}$$

which is equivalent to the first part of eq 1, may also decay by

(26) Cooper, J. W.; Manson, S. T. *Phys. Rev.* **1968**, *165*, 126.
(27) Cowan, R. D. *The Theory of Atomic Structure and Spectra*; CA, 1981.
(28) Yeh, J. J.; Lindau, I. *At. Data Nucl. Data Tables* **1985**, *32*, 1.
(29) Manson, S. T. *Adv. Electronics Electron Phys.* **1976**, *41*, 73.
(30) Bruhn, R.; Schmidt, E.; Schroder, H.; Sonntag, B. *J Phys. B* **1982**, *15*, 2807.
(31) Robin, M. B. *Chem. Phys. Lett.* **1985**, *119*, 33.
(32) Abbati, I.; Braicovich, L.; Carbone, C.; Lindau, I.; Nogami, J.; del Pennino, U.; Yeh, J. J. *Phys. Rev. B* **1985**, *32*, 5459.
(33) (a) Plummer, E. W.; Gustafsson, T.; Gudat, W.; Eastman, D. E. *Phys. Rev. A* **1977**, *15*, 2339. (b) Samson, J. A. R.; Gardner, J. L. *J. Elec. Spectrosc. Relat. Phenom.* **1976**, *8*, 35. (c) Collins, J. E.; Deluuche, J.; Lefebrve-Brion, M.; Leyli, B.; Nenner, L.; Hubin-Franskin, M. J.; Roy, P. R.; Raseev, G. *Stud. Phys. Theor. Chem.* **1985**, *33*, 33.

ejection of an electron localized mainly on the ligands. That the e_g* orbital is a covalent mix of ligand 5σ orbitals with metal *n*d orbitals provides one conceivable mechanism for this inter-channel coupling. Another consideration is that certain of the MOs giving rise to bands B, though principally ligand in character, have some metal d character as a result of overlap with the 1π and 5σ orbitals. It is noteworthy that in the spectrum of $Mo(CO)_6$ at the maximum of the *n*p → *n*d resonance ($h\nu$ = 48 eV; see Figure 2b) the central part of band B seems relatively more intense than it does at nonresonant energies suggesting association of the B resonance with a specific ion state, possibly the ^2E_g ion state with a hole in the e_g MO derived from the CO 5σ and Mo 4d orbitals, the super-Coster-Kronig decay being repesented in this case by

$$np^5e_g{}^4t_{2g}{}^6e_g{}^{*1} \rightarrow np^6e_g{}^3t_{2g}{}^6e_g{}^{*0} + e$$

For the Cr and W complexes, such a profile change in the B band is not apparent on visual examination of the spectra. Figure 11 shows branching ratios for each of the four separately integrated components of band B of $Mo(CO)_6$ as a function of the total B band intensities. It is evident from this figure that the component B_3 shows a reasonable correlation over the p → d resonance region with the branching ratios of band A (Figure 10b), whereas the ratios of B_1, B_2, and B_4 show no such correlation. The most likely explanation of this is that the ionization band from the e_g orbital is located within the IE region of component B_3. The e_g band is therefore assigned an IE of 14.8 eV, a value close to the original assignment.[6a]

The maxima found at 42 eV for the B bands of $Mo(CO)_6$ and $W(CO)_6$ seem metal independent although this is debatable as a similar maximum is not found for $Cr(CO)_6$. The value of 42 eV is close to the *n*p ionization thresholds of Mo and W (see Table I) and may be due to excitation of an *n*p electron to a CO localized level followed by decay and associated ejection of ligand electrons. This would be expected to be a weaker transition than *n*p → *n*d absorption due to the lower overlap of the metal p orbitals with ligand based wave functions.

As is apparent by inspection of Figures 5-7, the maxima in the RPPICS plots of the B bands are considerably smaller than those found for the A bands.

The C band show a maximum in cross-section at ca. 35 eV followed by a steady decline to higher photon energies similar to the RPPICS of the 4σ band of free CO (see Figure 9); again small resonance features may also be present.

Conclusions

It is clearly possible to distinguish between the strong *n*p → *n*d resonant photoemission shown by the metal d valence bands of the group VI hexacarbonyls and the rather weak structure shown by the ligand bands. Measurement of RPPICS as a function of photon energy over a range in which this excitation occurs thus provides a potential means of assignment of mainly metal d valence bands in the P.E. spectra of gas-phase molecules. The resonance phenomena are also apparent on examination of the branching ratios; indeed, they are so intense that they may be discerned by mere visual inspection of the spectra. In conclusion, it is seen that use of synchrotron radiation to determine RPPICS is likely to provide an invaluable assignment tool in UPS as well as providing crucial information about fundamental photoionization processes.

Acknowledgment. We thank Drs. J. B. West and F. Quinn for their role in setting up the UPS experiment at Daresbury and the SERC for financial support.

The Reactions of Electronically Excited Vinylidene Radicals with Molecular O_2

Askar Fahr[†] and Allan H. Laufer*[‡,§]

Contribution from the Chemical Kinetics Division, National Bureau of Standards, Gaithersburg, Maryland 20899, and the Chemical Sciences Division, Office of Basic Energy Sciences, U.S. Department of Energy, Washington, DC 20545. *Received November 21, 1986*

Abstract: The rate constant and mechanism for the reaction between electronically excited vinylidene ($H_2C{=}C)(^3B_2$) and molecular oxygen has been examined at 297 K. The vinylidene radicals were produced from the vacuum UV flash photolysis of vinyl chloride. Reactant triplet vinylidene and products CO and formaldehyde were observed, in real time, by their characteristic absorption in the vacuum UV region. The two products were formed in equal amounts, and the reaction probably proceeds through a cyclic intermediate. The rate constants for reaction of $D_2C{=}C(^3B_2)$ with molecular oxygen and $O(^3P)$ atoms were $(1.0 \pm 0.25) \times 10^{-13}$ and $(7 \pm 2) \times 10^{-11}$ cm^3 molecule^{-1} s^{-1}, respectively. The mechanism of the reaction of unsaturated hydrocarbon radicals with molecular O_2 is discussed.

Chemical reactions of small electronically excited hydrocarbon radicals, aside from those of the low-lying singlet methylene species, have not been extensively studied probably because these species are difficult to prepare and characterize. Methylene and CH, of course, are the smallest of the poorly investigated series of unsaturated hydrocarbon radicals. However, the existence and identification of a long-lived carbene, i.e., the electronically excited vinylidene radical ($H_2C{=}C$), has been documented in recent work from this laboratory.[1] In these earlier experiments the quenching of triplet vinylidene to the ground singlet state which in turn is quenched to ground-state acetylene has been examined for a series of nonreactive collision partners. Quenching by H_2 and CH_4 was also investigated. In these two cases there is the possibility of an exothermic abstraction reaction to produce a vinyl radical plus either an H atom or CH_3 radical.[2] Both reactions are predicted,

[†] National Bureau of Standards.
[‡] U.S. Department of Energy.
[§] Guest Worker at the Chemical Kinetics Division, U.S. National Bureau of Standards, Gaithersburg, MD 20899.

(1) Fahr, A.; Laufer, A. H. *J. Phys. Chem.* **1986**, *90*, 5064 and references therein.

(2) $\Delta H_f(H_2C{=}C)(^3B_2)$ = 141 kcal/mol based upon $\Delta H_f(H_2C{=}C)(^1A_1)$ = 100 kcal/mol (Davis, J. H.; Goddard, W. A., III; Harding, L. B. *J. Am. Chem. Soc.* **1977**, *99*, 2919) and a $(^1A_1)$-$(^3B_2)$ splitting of 41 kcal/mol (Osamura, Y.; Schaefer, H. F., III *Chem. Phys. Lett.* **1981**, *79*, 412). $\Delta H_f(C_2H_3)$ = 70.4 kcal/mol, $\Delta H_f(CH_3)$ = 35.1 kcal/mol (McMillan, D. F.; Golden, D. M. *Ann. Rev. Phys. Chem.* **1982**, *33*, 493).